JPPIPA 11(4) (2025)

Jurnal Penelitian Pendidikan IPA

http://jppipa.unram.ac.id/index.php/jppipa/index

Simulation of The Conductivity Hydraulic Effect on Seawater Intrusion

Ferdy[1*], Tirza Wungkana[1], Dolfie Paulus Pandara[1], Maria D. Bobanto[1], Hanny F. Sangian[1], Adey Tanauma[1], Seni H. Tongkukut[1], Hesky S. Kolibu[1]

[1]Departement of Physics, Faculty of Mathematics and Natural Sciences, Universitas Sam Ratulangi, Manado, Indonesia.

Received: September 22, 2024
Revised: January 21, 2025
Accepted: April 25, 2025
Published: April 30, 2025

Corresponding Author:
Ferdy
ferdysagita19@gmail.com

DOI: 10.29303/jppipa.v11i4.5437

Abstract: This research has been conducted with the aim of simulating the process of seawater intrusion using SEAWAT software and assessing the factors causing seawater intrusion. In this simulation, variations in hydraulic conductivity and aquifer material types are explored to understand their impact on the distribution of water levels. The simulation results are presented in the form of simulated concentration plots used to visualize concentration distribution with color gradients reflecting changes in concentration values. Additionally, the direction of groundwater flow is represented by arrows, aiding in understanding the movement patterns of dissolved substances within the aquifer. Simulated head plots are created using colors and contour lines. The resulting simulated head plots depict changes in color and contour lines that represent variations in water levels throughout the aquifer. Color gradients from yellow to purple indicate a decrease in water levels, while contour lines indicate the direction of groundwater flow. Furthermore, changes in the shape of contour lines from straight to curved depict changes in the topography or hydrogeological characteristics within the aquifer. The simulations are carried out by considering changes in hydraulic conductivity and aquifer material characteristics. In the context of this research, hydraulic conductivity is considered a key factor influencing the movement of dissolved substances within the aquifer, and through this analysis, it is found that hydraulic conductivity significantly affects water level distribution and groundwater flow patterns.

Keywords: Henry problem; Hydraulic conductivity; Seawater intrusion

Introduction

Benz et al. (2017) stated that several meters below our feet, shallow aquifers serve as a sustainable energy source and provide storage of freshwater and ecological habitats. Coastal aquifers establish a crucial hydrological connection between freshwater and seawater. These coastal aquifers serve as a vital water source for coastal areas in low-lying plains. Groundwater found in these coastal aquifers is frequently utilized for industrial purposes, food production, and household consumption (Pu et al., 2020). Submarine Groundwater Discharge (SGD) is an important factor for delivering nutrients to the coastal sea (Tamborski et al., 2020). An aquifer is an underground layer of permeable rock that contains water or other materials such as sand and gravel (Wals & Westra, 2015). According to Darsono & Darmanto (2019) groundwater is water stored in layers of soil or rock below the ground surface. Water that moves into the ground and is stored in the space between rock grains and combines to form a layer of soil called an aquifer. The aquifer layer is usually porous, permeable, and saturated, where this layer can not only drain water

How to Cite:
Ferdy, Wungkana, T., Pandara, D. P., Bobanto, M. D., Sangian, H. F., Tanauma, A., … Kolibu, H. S. (2025). Simulation of The Conductivity Hydraulic Effect on Seawater Intrusion. *Jurnal Penelitian Pendidikan IPA*, *11*(4), 795-810. https://doi.org/10.29303/jppipa.v11i4.5437

but also store water, for example unconsolidated sand, gravel, porous or cracked rocks.

An aquifer has two important functions, namely as a storage such as a reservoir and as a conduit of air such as a pipeline. Both functions are carried out by the pores or cavities in the aquifer rock. Two properties related to the function as storage are porosity, and density (specific yield) (Panguriseng, 2018). An aquifer consists of a single lithological unit, or several interrelated lithological units, which store and deliver water and are capable of supplying water to pumping wells. Aquifers are classified into two main types: confined aquifers that lie between two permeable retaining layers, and free aquifers in which the groundwater table, i.e., the interface between a fully filled and fully filled subsurface domain, forms the upper part of the aquifer boundary (Ajami, 2021).

Storms of air and runoff that infiltrate underground accumulate in permeable formations to form aquifers. Groundwater aquifers account for more than 60% of the freshwater supply and are the largest source of freshwater, providing a risk buffer to sustain critical air requirements during long, dry seasons. The erratic rainfall and aquifer recharge costs and abstraction patterns have profoundly changed the natural state of the aquifer. It is currently demonstrated that groundwater is over-pumped during droughts to compensate for surface water shortages, leading to serious groundwater depletion, with short and long term supply consequences (Shevah, 2014).

Groundwater is a primary reserve of freshwater and plays a significant role in freshwater supply systems, especially in coastal regions where 23% of the world's population resides within 100 kilometers of the coastline, relying on coastal groundwater (Pu et al., 2020).

Groundwater is a vital and basic need throughout the country. Several factors affect the quality of groundwater reservoirs, namely contamination by sea water intrusion (Harding, 1991). The increasing population and excessive groundwater extraction in coastal areas have led to various issues, one of which is seawater intrusion. Seawater intrusion is the process of seawater infiltrating into the groundwater aquifer, causing the mixing of freshwater with seawater (Damayanti, 2020). This intrusion poses a serious threat to groundwater resources (Bordbar et al., 2020). Seawater intrusion is a groundwater problem in coastal areas, because it has a direct impact on groundwater quality. As a result, changes occur in the quality and quantity of groundwater itself. Groundwater that was originally suitable for drinking water has decreased in quality so that it is not suitable for daily use (Ardaneswari et al., 2016).

The migration of saltwater into fresh aquifers through surface and subsurface flow pathways is known as saltwater intrusion (SWI). Seawater intrusion (SWI) is a major water security issue in coastal areas, and is exacerbated by changes in atmospheric, oceanic, and anthropogenic forcing. Subsurface lateral SWI, which is the onshore movement of freshwater-saltwater interfaces, occurs over timescales ranging from months to millennia and is caused by a decrease in the land-sea hydraulic gradient from pumping, decreased aquifer recharge, and sea-level rise (Werner et al., 2012). Lateral SWI has been extensively investigated due to its potential to degrade freshwater resources and degrade salt-intolerant coastal ecosystems (Cantelon et al., 2022).

Coastal aquifers at risk of seawater intrusion can lead to a decline in freshwater quality due to increased salinity. The contamination of these aquifers results in a reduction in groundwater resources, despite the fact that urban coastal areas with high population densities rely on groundwater for various purposes such as irrigation, drinking water, sanitation, and more. Many coastal aquifers in water-scarce areas are under pressure due to overexploitation, making it difficult for communities to access clean groundwater. Groundwater resources are a primary source of water supply for both humans and the natural environment within coastal aquifers. Continuous freshwater extraction can lead to severe degradation of coastal aquifers (Abd-Elaty et al., 2020).

The phenomenon of seawater intrusion is related to hydraulic conductivity, and hydraulic parameters, including hydraulic conductivity and porosity, play a crucial role in controlling flow characteristics and the transport of dissolved substances in porous media. In the case of the basic Henry problem, hydraulic conductivity is considered to be 864 m/day (Abd-Elaty et al., 2016). According to Mei et al. (2021), to study the impact of hydraulic conductivity on seawater intrusion, different hydraulic conductivity values are used depending on the type of rock material composing the aquifer. Hydraulic conductivity is affected by physical properties, namely porosity, grain size, grain arrangement, grain shape, and distribution. The range of intrinsic permeability values and hydraulic conductivity of rocks. The basic groundwater equations describe changes in groundwater hydraulic head over time and space. Hydraulic head is the potential pressure height of groundwater at a location within an aquifer. These equations encompass factors such as Darcy flow, hydraulic conductivity, and hydrostatic pressure differences.

Changes in cross-boundary layer permeability were found to cause seawater refraction and current separation, resulting in extensive mixing zones in low-permeability layers. Conversely, higher permeability layers cause flow lines to converge and produce narrower mixing zones (Lu et al., 2013). Because seawater is denser than freshwater, it infiltrates coastal aquifers and forms saltwater wedges. Along the freshwater-saltwater interface, salt diffuses into the freshwater zone, creating convective circulation through saltwater wedges.

The mixing zone between freshwater and seawater forms hotspots for water with varying chemical compositions. Seawater intrusion is generally caused by excessive aquifer exploitation, where groundwater extraction exceeds recharge, resulting in a decline in piezometric levels and rising sea levels influenced by climate change (Ouhamdouch et al., 2021). The Intergovernmental Panel on Climate Change (IPCC 2001) predicts that by 2100, global warming will lead to a sea-level rise of between 110 and 880 mm, and it is generally understood that sea-level rise is expected to result in the inland migration of the mixing zone between fresh and saline water (FAO 1997). This is because the rise in sea water levels leads to increased saline water heads at the ocean boundary, and enhanced sea water intrusion is the logical consequence (Werner & Simmons, 2009).

Syaifullah (2015) states that the sea surface temperature in the territory of Indonesia has a fairly wide range, namely 26.0 to 31.5°C. The temperature in the waters can be influenced by the position of the sun, geographical location, seasons and atmospheric conditions (Kalangi, 2013).

A confined aquifer is a seepage layer containing groundwater which is under pressure greater than free air pressure or atmospheric pressure, because the bottom and top of this aquifer are composed of an impermeable layer (usually clay) (Sarmauli et al., 2016). According to Fahs et al. (2018), to understand the process of seawater intrusion in coastal aquifers, the Henry Problem (HP) is often used and is an abstraction of seawater intrusion in vertical cross-sections of confined coastal aquifers perpendicular to the shoreline. The Henry Problem is considered a benchmark analysis for testing density-dependent groundwater flow models. It concerns a vertical cross-section through an isotropic, homogeneous, and bounded aquifer (Henry, 1964). The Henry Law Problem is related to hydraulic conductivity of seawater in the context of seawater intrusion. Essentially, the connection between the Henry Law Problem and hydraulic conductivity lies in how the hydraulic properties of porous media affect the movement and mixing of seawater and freshwater, which subsequently affects gas solubility according to Henry's Law (Diersch & Kolditz, 2002).

The distribution of salinity on the sea surface in Indonesian waters fluctuates greatly depending on the geographical structure, fresh water input from rivers, rainfall, evaporation and circulation of water masses. Seasonal changes also play an important role in changes in sea surface salinity in Indonesian waters (Suhana, 2018). According to Manginsela et al. (2016), in general, coastal sediments in Manado Bay are sand (46.7%), gravel sand (8.9%), silt sand (43.3%), and sandy mud (1.1%). The coastal conditions in Manado Bay are dominated by sand and mud sediments, which appear when the sea water recedes and in the northern part of Manado Bay there is also waste in the form of plastic waste, bottles, cans and other household waste (Posundu et al., 2019).

The main component in groundwater flow modeling is the distribution of hydraulic conductivity values. Hydraulic conductivity is the ability of a rock to flow groundwater at a certain speed. Hydraulic conductivity in fractured rocks has a higher complexity (degree of heterogeneity and anisotropy) compared to hydraulic conductivity in sedimentary rocks. The situation in the field, the hydroulic conductivity value has different values even in one rock layer (heterogeneous). The varying distribution of hydraulic conductivity is controlled by model validation and geological conditions (Cahyadi et al., 2014).

According to Pu et al. (2020), groundwater flow models are commonly used to simulate hydraulic flow patterns using three-dimensional models. MODFLOW is the most widely used software for numerical groundwater flow modeling, employing finite difference methods. MODFLOW is applied in groundwater simulation processes to address unsustainable issues and optimize system processes. According to Harbaugh (2005), MODFLOW is a standard code for the simulation of steady and transient groundwater flow in the subsurface, using a finite-difference approach to solve the three-dimensional flow equations or a rectangular grid. It allows for the simulation of representative subsurface conditions (e.g. heterogeneous hydraulic conductivities and transmissivities), as well as external stresses such as precipitation and flows through wells and drains. Additionally the SEAWAT version couples MODFLOW with the MT3DMS code the latter provides a multispecies transport model for the simulation of advection, dispersion, and sorption (Zhang et al., 2013). This coupling enables the simulation of groundwater flow with variable density and viscosity, and can be applied to study the transport of solutes and heat. This makes the SEAWAT version especially relevant for problems related to aquifer contamination (Thorne et al., 2006).

The influence of changing hydraulic parameters on seawater intrusion is studied using a numerical model

(SEAWAT) applied to the Henry Problem (Guo & Langevin, 2002; Lee, 2018). Henry (1964) presented an analytical solution for groundwater flow towards the coastline. Because an analytical solution is available for the Henry Problem, numerous numerical codes have been evaluated and tested against the Henry solution. Presented an analytical solution for groundwater flow towards the coastline. Because an analytical solution is available for the Henry Problem, numerous numerical codes have been evaluated and tested against the Henry solution (Simpson & Clement, 2004).

Methodology

The procedures in this study involve several steps. Firstly, data and parameters required for input and processing by the PyCharm software are collected and determined. To simplify the calculation process and save time, basic assumptions are added to the data and parameters, taking into consideration rational conditions as fundamental assumptions. Mathematical models for salinity and thermal transport are formulated based on the modeling approach by Hughes & Sanford (2004), which is derived from the Henry Problem. This approach is chosen for its simplicity, representation of real systems, and widespread use as a benchmark for understanding density-dependent groundwater flow. Numerical model formulation involves simulating solute transport through numerical solutions of mass balance equations for solutes and energy transport through numerical solutions of energy balance equations.

Modeling is conducted using SEAWAT software for groundwater flow and MODFLOW for simulating groundwater intrusion effects. The USGS developed the Seawater Intrusion Package 2 (SWI2), compatible with MODFLOW version 6 (Bakker et al., 2013), which has been installed in PyCharm. Parameters and data are inputted into the software for computational processing.

Result and Discussion

Hydraulic Conductivity Variation on Salinity Distribution

The analysis of hydraulic conductivity variation on the distribution of salinity concentration involves evaluating the patterns and changes in salinity distribution within the system based on hydraulic conductivity variations. By utilizing SEAWAT and MODFLOW software, the simulation results can be analyzed to understand their effects. Based on research conducted using PyCharm software, the parameter values used are secondary data extracted from relevant research journals, including the hydraulic conductivity values of different types of rocks within the aquifer. Thermal parameters used were selected from previous studies, the values for longitudinal and transverse dispersions that depend on the scale were chosen from (Hunt et al., 2011).

The output generated consists of plotted graphs depicting the aquifer's conditions, groundwater flow patterns, flow rates, seawater intrusion, and the interface or mixing zones between seawater and freshwater. Out of the 14 input data sets run through the software, each data set produces 2 plots, resulting in a total of 28 plotted graphs. To facilitate understanding, we will discuss them according to clusters of hydraulic conductivity values defined as 100-500, 1-99, 0.1-0.99, and 0.01-0.099 m/day.

These plots display simulation results of concentrations at the end of the simulation. On the x-axis, the horizontal distance (column coordinate) within the model is displayed, with a fixed value of $Lx = 2.0$ m. On the y-axis, the vertical distance (depth) within the model is displayed, with a value of $Lz = 1.0$ m. On the right side of the plot, there is a color variation indicating salinity concentrations ranging from 0.0 to 17.5 ppt. The color matrix represents the distribution of seawater concentration within the aquifer. The more intensive the blue color, the higher the concentration.

These plots also show vectors of horizontal and vertical water flow (qx, qy, qz) indicated by white arrows. The length of the arrows represents the velocity of water flow, while their direction indicates the flow direction. Water flow patterns refer to the direction and speed of water flow within the hydrological system, such as rivers, lakes, or groundwater aquifers. Arrows on the simulated concentration plots are typically used to indicate the direction of concentration flow within the system. These arrows provide information about how the concentration of a particular substance or component moves within water or other media.

In the context of simulating the concentration of seawater or other substances in seawater using software like SEAWAT, arrows can be used to depict the flow patterns of seawater concentration within the groundwater aquifer. For example, if the simulation depicts seawater intrusion into the aquifer, the arrows may point in the direction indicating the flow of seawater from the seawater source toward areas affected by intrusion. These arrows help visualize the movement of seawater concentration and provide an overview of how seawater flows through the aquifer and affects the water quality within it.

Water flow patterns are greatly influenced by topography, hydrogeological properties, and boundary conditions within the system. In the case of groundwater aquifers, water flow patterns can be understood through numerical simulations using hydrogeological modeling software like MODFLOW.

The color scale displayed on the simulated concentration plots ("Simulated Concentrations") is used to provide information about the range of concentration values observed in the simulation. This color scale is usually included in the plot as a color bar. A color bar is a scale of colors displayed alongside the plot to provide reference to the numerical values corresponding to each color on the plot. Color bars are used to provide a visual understanding of the range of concentration values generated by the simulation. On the color scale, there is typically a gradient of colors from one end to the other. For example, in a plot of seawater concentration, the color scale may start with dark purple representing low concentration, then transition to dark blue, light blue, turquoise, green, and finally yellow representing higher concentrations. The color scale on the color bar is accompanied by numeric labels indicating the concentration values corresponding to each color. These labels assist in interpreting and understanding the range of concentrations observed in the simulation. This color bar helps track concentration change patterns and compare concentration values in different parts of the model. In Figure 4.1, you can see cluster (a) within the range of 100-500 m/day.

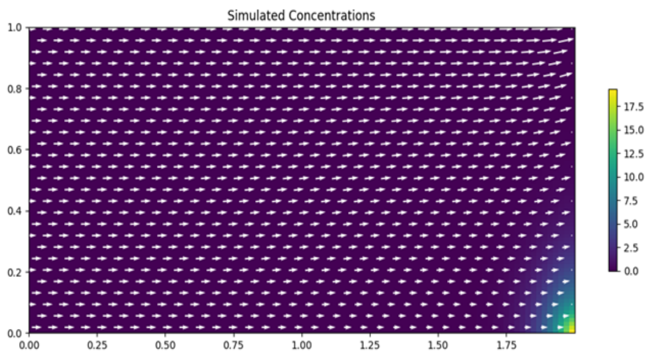

(a)

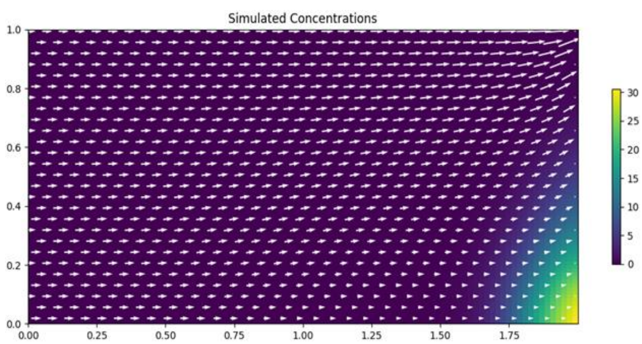

(b)

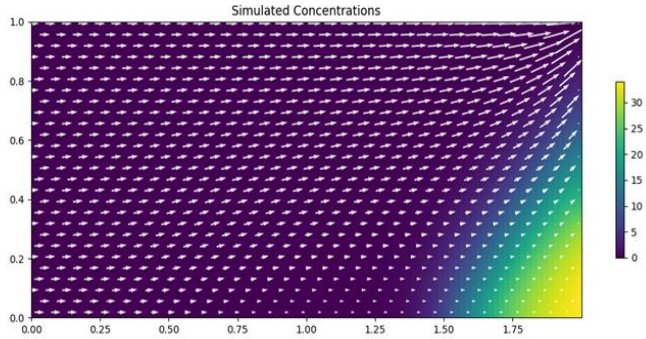

(c)

Figure 1. Cluster (a) Hydraulic conductivity 100 - 500 m/day (Source: PyCharm 2022)

In the figure resulting from running several data clusters (a), consisting of three types of materials, namely coarse gravel, medium gravel, and fine gravel, which have been input into the software, different plotted graphs are obtained for each hydraulic conductivity value entered. It can be observed that these three graphs have specific differences, including varying amounts of seawater entering the aquifer, different flow rates of water, and differences in the scale on the color bar.

In Figure (a), which represents an aquifer composed of coarse gravel with a hydraulic conductivity value of 150 m/day, it can be concluded that there is minimal or almost no seawater intrusion. It can be seen at x = 1.981 m and y = 0.009 m that intrusion occurs with salinity concentrations in the range of ≥ 17.5 ppt, while the distribution of salinity concentrations.

With the interface or mixing zone extends up to x = 1.799 m and y = 0.28 m, with salinity concentrations ranging from 2.5 to 15.0 ppt. The flow rate of water within the aquifer is initially normal and then begins to increase at x = 1.430 m and y = 0.995 m, while it decreases at x = 1.169 m and y = 0.172 m.

In Figure (b), generated from running data by changing the aquifer constituents to medium gravel, with a hydraulic conductivity value of 270 m/day, it can be seen that seawater intrusion into the aquifer is greater compared to coarse gravel. In this plot, it can be explained that the colorbar values next to the plot have a different scale from the previous one, ranging from 0 ppt to 30 ppt. Seawater intrusion occurs at x = 1.977 m and y = 0.051 m with salinity concentrations ≥ 30 ppt, while the distribution of salinity concentrations with the interface or mixing zone extends up to x = 1.657 m and y = 0.551 m, with salinity concentrations ranging from 5 to 25 ppt. The flow rate is initially normal and begins to increase at x = 1.186 m and y = 0.997 m, while it decreases at x = 0.879 m and y = 0.167 m.

In Figure (c), it is explained that from the results of running data with hydraulic conductivity values of fine gravel with a value of 450 m/day, it can be seen that seawater intrusion is even greater than in aquifer conditions with medium and coarse gravel as the constituent materials. The colorbar in this plot has the same scale as that of medium gravel, starting from 0 to 30 ppt. Seawater intrusion into the aquifer in this condition occurs at x = 1.938 m and y = 0.059 m with salinity concentrations ≥ 30 ppt, while the distribution of salinity concentrations with the interface or mixing zone extends up to x = 1.402 m and y = 0.796 m, with salinity concentrations ranging from 5 to 25 ppt. The flow rate is initially normal and begins to increase at x = 0.811 m and y = 0.958 m, while it decreases at x = 0.739 m and y = 0.242 m.

From the three plots in Figure Cluster (a), it can be concluded that if the hydraulic conductivity value is low, the water flow within the model can be limited or slow. This can result in more localized and uneven distribution of water concentration. If water flow is limited, there may be little horizontal movement of water, and this can affect the pattern and direction of concentration flow. In the plot, this can be seen with unclear flow directions or short and weak flow vectors. This can affect the ability of freshwater to resist or prevent seawater intrusion. Conversely, if the hydraulic conductivity value is high within the aquifer, it will allow for strong freshwater flow. Strong freshwater flow can generate higher hydrostatic pressure and prevent seawater intrusion.

Based on Figure 2, In Figure (a), with a hydraulic conductivity of 45 m/day, seawater intrusion occurs at x = 1.980 m and y = 0.099 m with salinity concentration ≥ 1.75 ppt. The distribution of salinity concentrations with the interface or mixing zone extends up to x = 1.660 m and y = 0.950 m, with salinity concentrations ranging from 0.25 to ≥ 1.50 ppt. The flow rate is normal, with no increase, but there is a decrease at x = 1.942 m and y = 0.017 m.

In Figure (b), representing medium sand with a hydraulic conductivity value of 12 m/day, it can be observed that seawater intrusion into the aquifer is greater than in the previous image. Seawater intrusion in this condition occurs at x = 1.984 m and y = 0.190 m with salinity concentrations ≥ 1.0 ppt, while the distribution of salinity concentrations with the interface or mixing zone extends up to x = 1.656 m and y = 0.999 m, with salinity concentrations ranging from 0.2 to ≥ 1.0 ppt. The flow rate is normal, with no increase or decrease.

Figure (c) depicts fine sand as the aquifer's constituent material with a hydraulic conductivity value of 2.5 m/day. It can be seen that seawater intrusion into the aquifer is predominantly vertical. Seawater intrusion occurs at x = 1.988 m and y = 0.580 m with salinity concentrations ≥ 1.0 ppt. The distribution of salinity concentrations with the interface or mixing zone extends up to x = 1.601 m and y = 0.999 m, with salinity concentrations ranging from 0.1 to ≥ 1.0 ppt. The flow rate in this condition is normal, with no increase or decrease.

In Figure (d), generated from running data by changing the aquifer's constituent material to dune sand with a hydraulic conductivity value of 20 m/day, it can be observed that seawater intrusion into the aquifer is not significant. Seawater intrusion occurs at x = 1.997 m and y = 0.012 m with salinity concentrations ≥ 1.0 ppt, while the distribution of salinity concentrations with the interface or mixing zone extends up to x = 1.560 m and y = 1.00 m, with salinity concentrations ranging from 0.1 to ≥ 1.0 ppt. The flow rate is normal, with no increase or decrease.

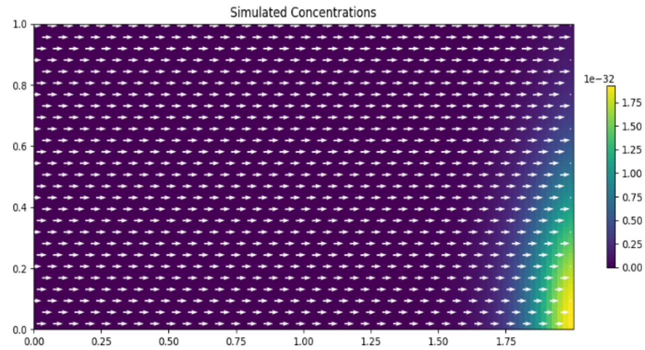

(a)

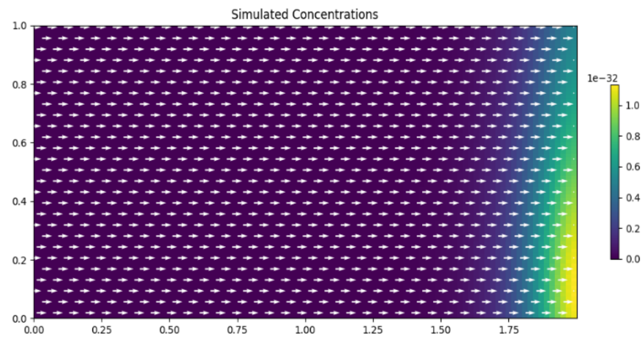

(b)

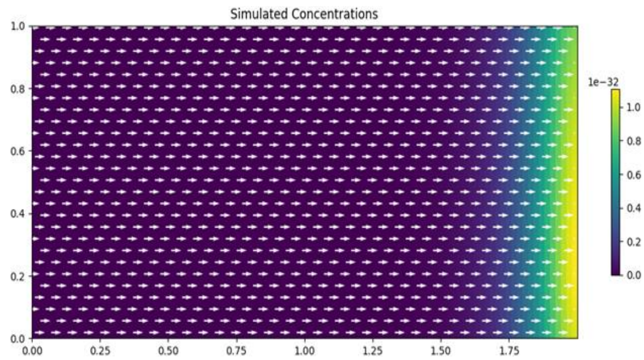

(c)

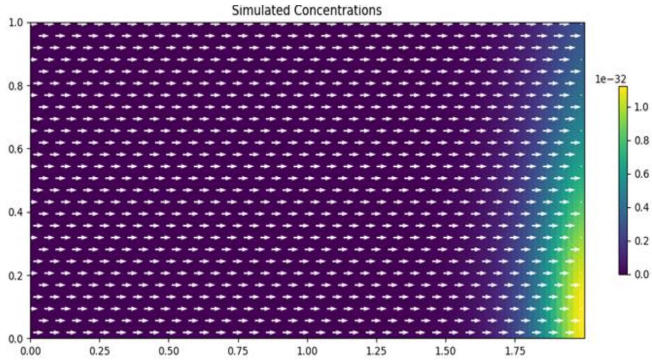

(d)

Figure 2. Cluster (a) Hydraulic conductivity 100 - 500 m/day (Source: PyCharm 2022)

In the figure for cluster (b) representing hydraulic conductivity in the range of 1-99 m/day, the plotted graphs resulting from running data with various aquifer material types, including coarse sand, medium sand, fine sand, and dune sand, show different outcomes. The colorbar scales for medium sand, fine sand, and dune sand are similar, starting from 0.0 to 1.0 ppt, whereas for medium sand, the colorbar scale is different, starting from 0.00 to 1.75 ppt.

Based on the results of the four graphs in the 1-99 m/day cluster, each with different hydraulic conductivity values, it can be concluded that the smaller the hydraulic conductivity value of the aquifer material or the closer it is to zero, the greater the likelihood of seawater intrusion. However, in this condition, seawater intrudes vertically into the aquifer. Conversely, for aquifers with constituent materials having values above 10, the likelihood of seawater intrusion is low. There is no significant difference in the interface or mixing zone between freshwater and saline water in all four graphs, as the interface zone stops or only extends to around x = 1.500 m.

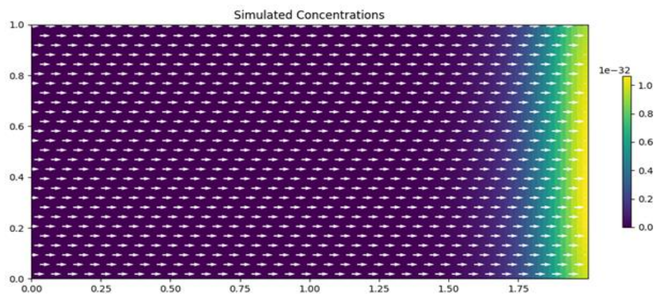

(a)

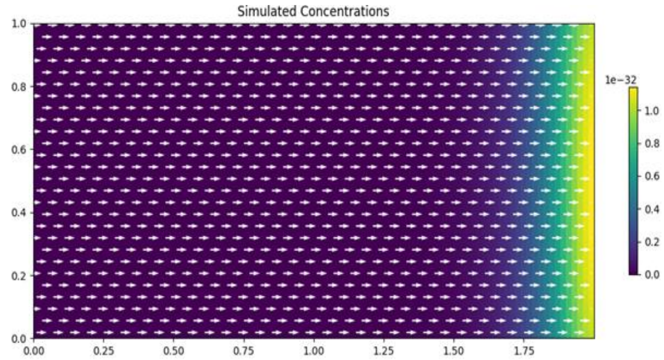

(b)

Figure 3. Cluster (c) Hydraulic conductivity 0.1 - 0.99 m/day (Source: PyCharm 2022)

In Cluster (c), there are four hydraulic conductivity values, including three types of materials with the same value of 0.2 m/day, which are fine-grained sandstone, tuff, and weathered gabbro. Because they have the same value, only one plotted graph is displayed. For one different material type, limestone with a hydraulic conductivity of 0.94 m/day is included. In Figure (a), representing hydraulic conductivity with a value of 0.2 m/day, it can be seen that the largest seawater intrusion into the aquifer is encountered in the middle part. In this plot, it can be explained that the colorbar values next to the plot have a scale starting from 0.0 to 1.0 ppt. Seawater intrusion occurs at x = 1.980 m and y = 0.300 - 0.700 m with salinity concentrations ≥ 1.0 ppt, while the distribution of salinity concentrations with the interface or mixing zone extends up to x = 1.559 m and y = 1.00 m, with salinity concentrations ranging from 0.1 to ≥ 1.0 ppt. The flow rate is normal, with no increase or decrease in the aquifer.

In Figure (b), the aquifer's constituent material is limestone with a hydraulic conductivity value of 0.94 m/day. Seawater entering the aquifer is found in the middle part at x = 1.992 m and y = 0.238 - 0.637 m with salinity concentrations ≥ 1.0 ppt, while the mixing zone or interface can be found up to x = 1.540 m and y = 1.00 m, with salinity concentrations ranging from 0.1 to ≥ 1.0 ppt. The flow rate in this condition is normal.

From these two graphs, it can be observed that saline water enters the aquifer from the middle portion, and intrusion in these two conditions is quite high due to the low hydraulic conductivity values, causing limited water flow in the model. This uneven distribution of water concentration can affect the ability of freshwater to resist or prevent seawater intrusion.

Based on Figure 4, in Cluster (d), there are four different hydraulic conductivities: silt with a hydraulic conductivity of 0.08 m/day, clay with 0.0002 m/day, dolomite with 0.001 m/day, and basalt with 0.01 m/day. The first plotted graph in Figure (a) represents hydraulic conductivity with a value of 0.08 m/day. It can be observed that the largest intrusion of seawater into the aquifer occurs in the middle section. In this plot, the colorbar values next to the plot are scaled from 0.0 to 1.0 ppt. Seawater intrusion occurs at x = 1.990 m and y = 0.273 - 0.747 m, with salinity concentrations ≥ 1.0 ppt, while the distribution of salinity concentrations with the interface or mixing zone extends up to x = 1.540 m and y = 1.00 m, with salinity concentrations ranging from 0.1 to ≥ 1.0 ppt. The flow rate is normal, with no increase or decrease in the aquifer.

In Figure (b), the aquifer is composed of clay with a hydraulic conductivity value of 0.0002 m/day. Seawater entering the aquifer is found in the middle section at x = 1.983 m and y = 0.278 - 0.774 m, with salinity concentrations ≥ 1.0 ppt, while the mixing zone or interface can be found up to x = 1.559 m and y = 1.00 m, with salinity concentrations ranging from 0.1 to ≥ 1.0 ppt. The flow rate in this condition is normal.

Plot Figure (c) represents an aquifer with dolomite as the constituent material with a hydraulic conductivity value of 0.001 m/day. Seawater entering the aquifer is found in the middle section at x = 1.997 and y = 0.249 - 0.649, with salinity concentrations ≥ 1.0, while the mixing zone or interface can be found up to x = 1.540 and y = 1.00, with salinity concentrations ranging from 0.1 to ≥ 1.0. The flow rate in this condition is normal.

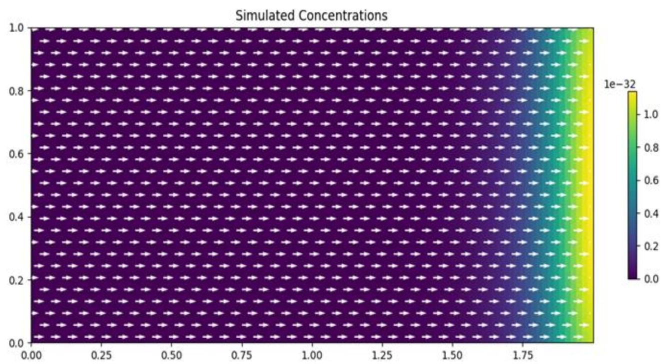

(a)

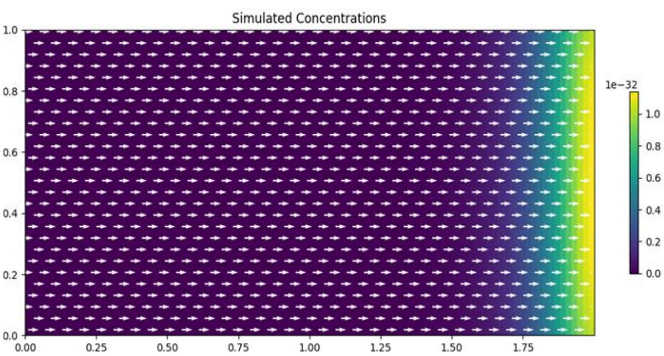

(b)

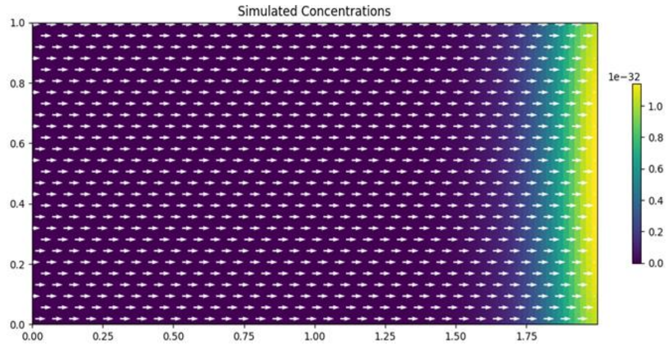

(c)

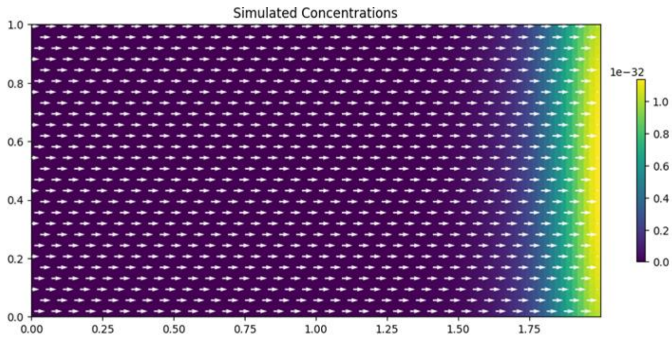

(d)

Figure 4. Cluster (d) Hydraulic conductivity 0.01 – 0.099 m/day (Source: PyCharm 2022)

Plot Figure (d) represents an aquifer with basalt as the constituent material with a hydraulic conductivity value of 0.01 m/day. Seawater entering the aquifer is found in the middle section at x = 1.990 m and y = 0.249 - 0.750 m, with salinity concentrations ≥ 1.0 ppt, while the mixing zone or interface can be found up to x = 1.540 m and y = 1.00 m, with salinity concentrations ranging from 0.1 to ≥ 1.0 ppt. The flow rate in this condition is normal.

From these four images, it can be seen that saline water enters the aquifer from the central portion, and intrusion in these four conditions is quite high due to the low hydraulic conductivity values, resulting in limited water flow in the model. This can lead to uneven distribution of water concentration and affect the ability of freshwater to resist or prevent seawater intrusion. If the flow vector points from freshwater to saltwater, it indicates the movement of freshwater into the saltwater zone. In the context of hydrogeology, this can occur when there is a drop in the groundwater level or an increase in hydrostatic pressure on the freshwater flowing toward the saltwater zone. The movement of freshwater into saltwater has significant implications for water quality and water resource management. Seawater intrusion into groundwater aquifers can lead to increased salinity and damage the quality of available freshwater. Therefore, understanding and modeling the movement of freshwater and saltwater in hydrogeological simulations are crucial for managing and protecting underground water resources. The movement of freshwater toward saltwater can occur in several situations, including a drop in the groundwater level. In such conditions, if the groundwater level decreases, freshwater can move from the freshwater zone to the saltwater zone to achieve hydrostatic equilibrium. This can occur due to excessive groundwater extraction, drought, or other human activities that affect the groundwater level. Seawater intrusion occurs when seawater enters the freshwater zone due to differences in density and hydrostatic pressure. If the flow of freshwater is not strong enough to prevent seawater intrusion, freshwater can be pushed toward the saltwater zone.

Variation in Hydraulic Conductivity and its Impact on Head Distribution

The Simulated Heads Plot displays the simulation results of groundwater levels within the aquifer at the end of the simulation. On the x-axis, the horizontal distance (column coordinates) within the model is presented, while the y-axis represents the vertical depth within the model. The color matrix depicts the distribution of groundwater levels within the aquifer. The unit of measurement for the values displayed on the colorbar alongside the simulated heads plot is in "meters" or "m". In the context of groundwater head simulation, the colorbar indicates the range of groundwater levels in meters. Higher values on the colorbar correspond to greater depths of water within the aquifer. Additionally, this plot displays contour lines of groundwater levels represented by white lines with numerical values printed above the contours.

The "Simulated Heads" plot serves as a visualization that illustrates the distribution of groundwater levels (head) generated by the hydrogeological model simulation at the conclusion of the simulation. This plot provides insights into how groundwater levels within the aquifer change and are distributed across the entire model area. The distribution of groundwater levels is depicted in the form of a map or image that reflects the conditions at the end of the simulation. The matrix containing the values of groundwater levels in each cell is plotted using a specific color scale. The plot is accompanied by a colorbar, which assists in mapping numerical values of groundwater levels to corresponding colors. The colors on this scale represent the range of observed groundwater levels during the simulation. For instance, lighter blue may represent shallow groundwater levels, while darker red may represent deeper groundwater levels. Some "Simulated Heads" plots also include contour lines or isopotential lines that connect points with the same groundwater level. These lines aid in visualizing the contours and patterns of groundwater level changes within the model. Numerical labels on the contour lines provide specific values of groundwater levels at particular points. These labels are helpful in interpreting groundwater levels in specific areas within the model.

Based on Figure 5 (a), the simulation results of "Simulated Heads" with coarse gravel as the aquifer material reveal an interesting distribution of groundwater levels within the hydrogeological model. The plot shows a color gradient from the highest groundwater level of approximately 0.06 meters (yellow) to the lowest groundwater level of about 0.00 meters (purple). The color yellow indicates higher groundwater levels, while shades of purple indicate lower groundwater levels. The contour lines in the plot exhibit varying patterns; straight contour lines transitioning from yellow to dark green signify zones with higher groundwater levels that tend to be relatively flat or gently sloping. For example, along the x-axis from 0.00 to 0.50 meters, there is a zone with a groundwater level of around 0.06 meters, which appears to be relatively flat. However, when contour lines begin to curve from dark green to dark purple, it indicates sharper changes in groundwater levels. For instance, along the x-axis from 1.00 to 1.75 meters, the contour lines form complex patterns, signifying differences in topography or distinct hydrogeological conditions in that area. Complex contour patterns can suggest more intricate groundwater flow or the presence of water sources influencing the distribution of groundwater levels.

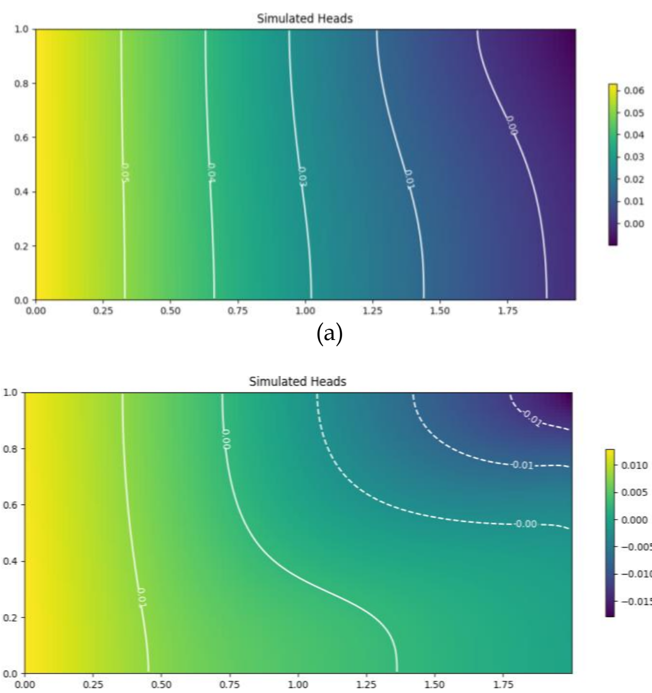

(a)

(b)

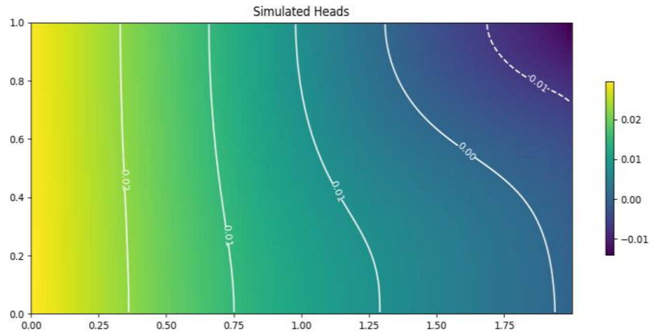

(c)

Figure 5. Simulated heads plot cluster (a) (Source: PyCharm 2022)

Simulated Heads Plot Cluster (b), the results of the "Simulated Heads" simulation for medium gravel material display an intriguing distribution of groundwater levels within the hydrogeological model. This plot exhibits a color gradient from groundwater levels of approximately 0.02 meters (yellow) to 0.01 meters (green), then approximately 0.01 meters (turquoise) to 0.00 meters (dark green), and finally reaching around -0.01 meters (dark blue) to -0.01 meters (purple). On the x-axis, the values used are 0.00, 0.25, 0.50, 0.75, 1.00, 1.25, 1.50, and 1.75 meters. Straight contour lines transitioning from yellow represent zones with higher groundwater levels that tend to be relatively flat. However, when contour lines slightly bend in light green, it indicates more pronounced changes in groundwater levels, possibly signifying differences in topography or distinct hydrogeological conditions in that area. As contour lines curve further from dark green to dark purple, it suggests a more complex pattern in the distribution of groundwater levels. Dashed contour lines observed in dark blue to purple (-0.01 meters) indicate areas with lower groundwater levels compared to their surroundings.

Simulated Heads Plot Cluster (c), the simulation results for fine gravel and pebbles as the aquifer material with a hydraulic conductivity value of 450 m/day are depicted in this plot. The plot illustrates a color gradient from groundwater levels of approximately 0.010 meters (yellow) to 0.005 meters (green), then 0.000 meters (turquoise), further reaching around -0.005 meters (dark green) to -0.010 meters (dark blue), and finally approximately -0.015 meters (purple). On the x-axis, the values used are 0.00, 0.25, 0.50, 0.75, 1.00, 1.25, 1.50, and 1.75 meters. The contour lines on the plot exhibit intriguing patterns; straight contour lines transitioning from yellow represent zones with higher groundwater levels that tend to be relatively flat. However, when contour lines slightly bend in light green, it indicates more pronounced changes in groundwater levels. As contour lines curve further from dark green to dark purple, it suggests a more complex pattern in the distribution of groundwater levels. Dashed contour lines observed in dark green to purple on the plot indicate areas with relatively sharp changes in groundwater levels. These dashed contour lines are typically used to mark significant differences in groundwater levels between adjacent contour lines. In regions with dashed contour lines, the changes in groundwater levels between one contour line and the next are relatively larger compared to areas with straight contour lines. This may indicate the presence of different hydrogeological features or hydrological boundaries affecting groundwater flow in that area. For example, dashed contour lines may represent the boundary between aquifer zones with different hydraulic conductivity or transition zones between freshwater and saline water (freshwater-saltwater interface) known as the saltwater intrusion zone.

Based in Figure 6, the groundwater flow patterns in the simulation heads for coarse sand, as shown in Figure (a), depict a variation in groundwater elevation throughout the model domain. The colors on the plot range from yellow (0.20 m) to shades of purple (0.03 m), representing the variations in groundwater elevation across the model. Higher values (yellow) indicate areas with higher groundwater elevation, approximately 0.20 meters, while lower values (purple) indicate areas with lower groundwater elevation, around 0.03 meters. The color gradient from yellow (0.20 m) to dark green (0.16 m) and purple (0.03 m) signifies decreasing groundwater elevation along the y-axis. This shows that groundwater levels decrease as you move from the top to the bottom of the model.

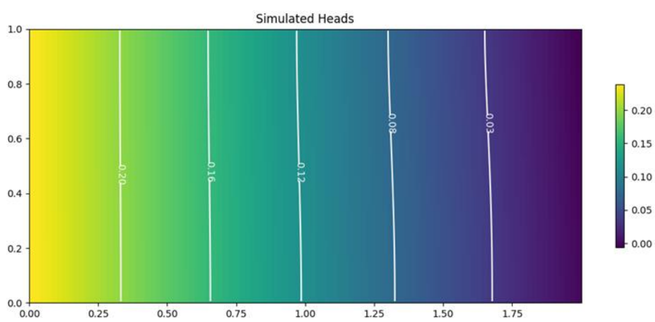

(a)

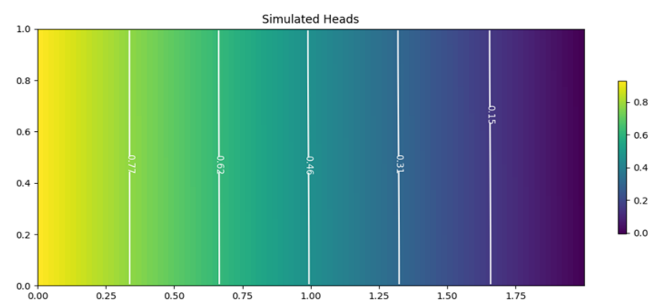

(b)

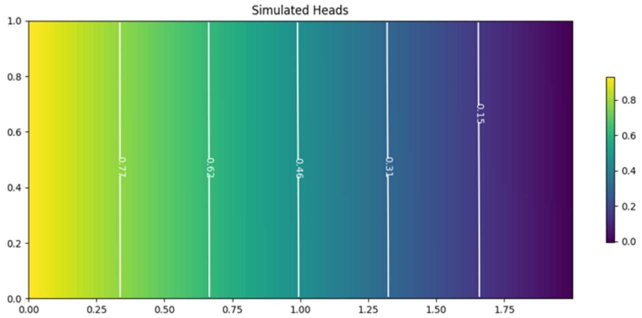

(c)

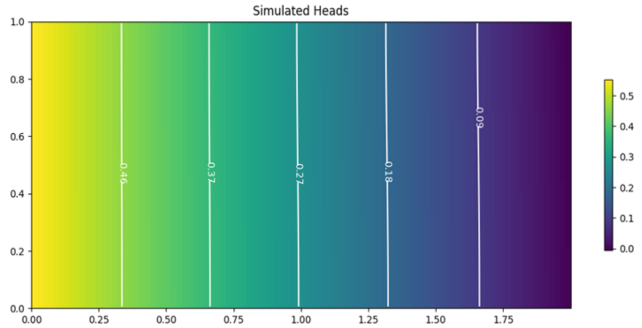

(d)

Figure 6. Simulated heads plot cluster (b) (Source: PyCharm 2022)

Straight contour lines from yellow to turquoise (0.12 m) indicate regions with relatively constant groundwater elevation at the top of the model but then start to curve slightly at the bottom (along the y-axis) in dark green (0.08 m) to dark purple (0.03 m). This suggests a sharper difference in groundwater elevation at the bottom of the model, ranging from about 0.12 meters at the top to 0.03 meters at the bottom. The change in contour line shape from straight to curved indicates a more complex groundwater flow pattern at the bottom of the model, which may be influenced by topography, geological structure, or hydrogeological heterogeneity.

In Figure (b), the groundwater flow patterns in the simulation heads for mound sand material display an intriguing distribution of groundwater elevation within the hydrogeological model. The colors on the plot range from yellow (0.46 m) to shades of purple (0.09 m), representing the variations in groundwater elevation across the entire model domain. Higher values (yellow) indicate areas with higher groundwater elevation, approximately 0.46 meters, while lower values (purple) indicate areas with lower groundwater elevation, around 0.09 meters. The color gradient from yellow (0.46 m) to green (0.37 m) and purple (0.09 m) signifies a decreasing trend in groundwater elevation along the y-axis. Thus, it is evident that groundwater levels consistently decrease from the top to the bottom of the model.

Straight contour lines from yellow to dark purple indicate regions with relatively constant groundwater elevation throughout the model, but groundwater elevation continues to decrease overall from the top to the bottom of the model. The ability of contour lines to remain straight suggests that the groundwater flow pattern in this mound sand type is generally more consistent and stable across the entire model domain.

Figure (c) depicts the distribution of groundwater elevation within the medium sand type aquifer with a hydraulic conductivity of 12 m/day. On the plot, the color gradient ranges from yellow (0.77 m) to green (0.62 m), then turquoise (0.46 m) to dark green to dark blue (0.31 m), and finally to shades of purple (0.15 m), representing variations in groundwater elevation throughout the hydrogeological model. Higher groundwater elevations are shown with brighter colors, while lower groundwater elevations are depicted with darker colors. From this plot, it is evident that the highest groundwater elevation (0.77 m) is on the left side of the model, while the lowest groundwater elevation (0.15 m) is on the right side of the model.

Dashed contour lines from yellow (0.77 m) to shades of purple (0.15 m) indicate areas with lower groundwater elevation compared to their surroundings. Straight contour lines indicate that the groundwater flow pattern in this medium sand type is generally consistent and stable across the entire model domain. Using the x and y axes, you can observe the spatial distribution pattern of groundwater elevation within the hydrogeological model. The x-axis represents horizontal locations, while the y-axis represents vertical depths within the model.

Figure (d) illustrates the distribution of groundwater elevation in the aquifer with medium sandstone material and a hydraulic conductivity of 3.1 m/day. On the plot, the color gradient ranges from yellow (3.02 m) to green (2.42 m), then turquoise (1.81 m) to dark green to dark blue (1.21 m), and finally to shades of purple (0.60 m), representing variations in groundwater elevation within the hydrogeological model. From this plot, it is evident that the highest groundwater elevation (3.02 m) is at the top, while the lowest groundwater elevation (0.60 m) is at the bottom. Straight contour lines from yellow (3.02 m) to shades of purple (0.60 m) indicate that the groundwater flow pattern in this medium sandstone type is generally consistent and stable across the entire model domain.

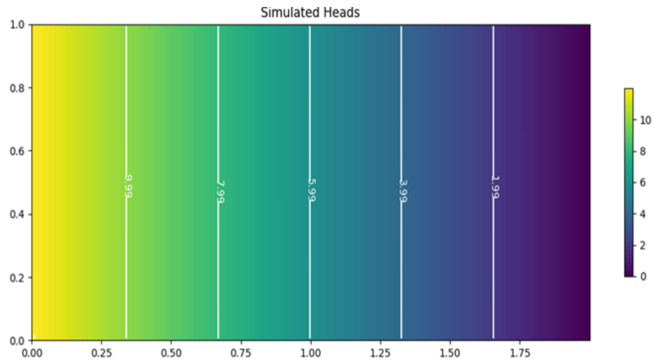

(a)

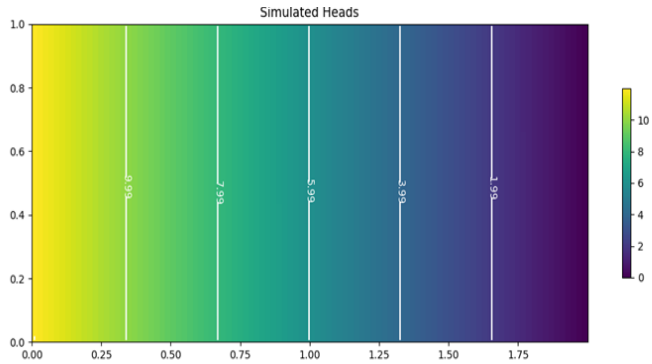

(b)

Figure 7. Simulated heads plot cluster (c) (Source: PyCharm 2022)

In Cluster (c), the heads simulation covers a range of hydraulic conductivity values ranging from 0.1 to 0.99 m/day. Within this range, there are four distinct hydraulic conductivity values. Among the four types of aquifer material, three have the same hydraulic conductivity value, which is 0.2 m/day. Therefore, only two plot images are displayed because the results of the plots for these three materials are identical.

In Figure (a), it illustrates the distribution of groundwater elevation within the fine-grained sandstone material with a hydraulic conductivity of 0.2 m/day. On the plot, the color gradient ranges from yellow (47.01 m) to green (37.61 m), then to turquoise (28.21 m), dark green to dark blue (18.80 m), and finally to shades of purple (9.40 m). These colors represent variations in groundwater elevation across the entire hydrogeological model. From this plot, it is evident that the highest groundwater elevation (47.01 m) is on the left side of the model, while the lowest groundwater elevation (9.40 m) is on the right side. Straight contour lines indicate that the groundwater flow pattern in this fine-grained sandstone material tends to be consistent and stable across the entire model domain.

Figure (b) depicts the distribution of groundwater elevation within limestone material with a hydraulic conductivity of 0.94 m/day. On the plot, the color gradient ranges from yellow (9.99 m) to green (7.99 m), then to turquoise (5.99 m), dark green to dark blue (3.99 m), and finally to shades of purple (1.99 m). These colors represent variations in groundwater elevation across the entire hydrogeological model. From this plot, it is evident that the highest groundwater elevation (9.99 m) is on the left side of the model, while the lowest groundwater elevation (1.99 m) is on the right side. Straight contour lines indicate that the groundwater flow pattern in this limestone material tends to be consistent and stable across the entire model domain.

Based on Figure 8, in the fourth plot cluster (d), the groundwater elevation values are very high due to the low hydraulic conductivity. When hydraulic conductivity is low, groundwater flow is impeded, and water tends to get trapped within the rock formation or aquifer. As a result, groundwater elevation within the model can become very high because water cannot flow out of the system rapidly. This high groundwater elevation can occur in specific areas with unique hydrogeological conditions, such as highly dense or impermeable sedimentary rock deposits, as exemplified by the four simulated material types: clay, basalt, dolomite, and silt.

Figure (a) shows that fine-grained silt material significantly influences the distribution of groundwater elevation in the hydrogeological model. On the plot, the color gradient ranges from yellow (177.55 m) to green (94.04 m), turquoise (70.53 m), dark green (47.02 m), and shades of purple (23.51 m), indicating interesting changes in groundwater elevation. Straight contour lines from yellow to purple indicate a relatively consistent and flat distribution of groundwater elevation in the model. Higher groundwater elevations are represented by yellow colors, while lower elevations are represented by purple colors. The x and y axes on the plot indicate locations within the model, and their values influence the distribution of groundwater elevation in the model. Additionally, the values on the colorbar beside the plot, namely 0, 20, 40, 60, 80, 100, 120, and 140 m, indicate the elevation scale in relevant units, which is meters.

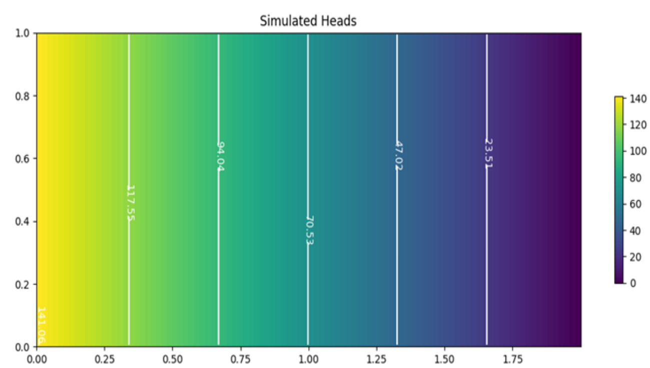

(a)

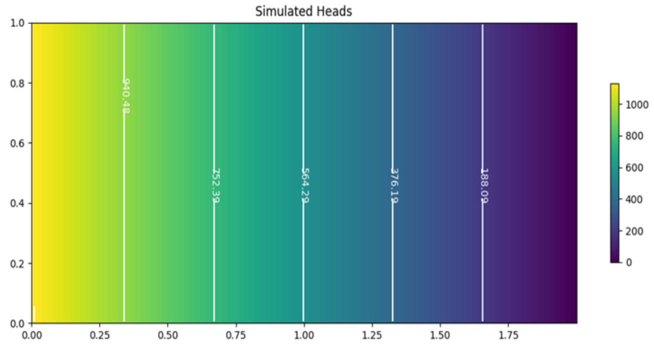

(b)

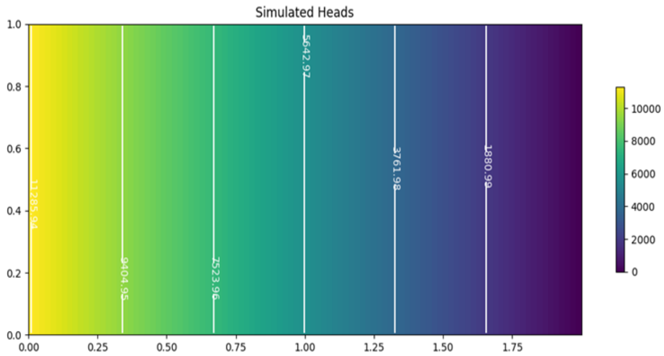

(c)

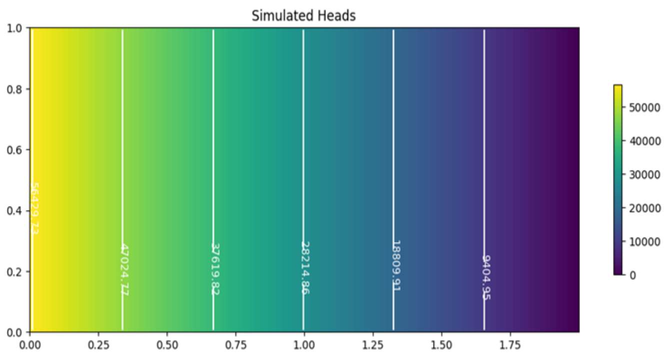

(d)

Figure 8. Simulated heads plot cluster (d) (Source: PyCharm 2022)

Figure (b) shows that basalt material influences the distribution of groundwater elevation in the model. On the plot, the color gradient ranges from yellow (940.48 m) to green (752.39 m), turquoise (564.59 m), dark green (376.19 m), and shades of purple (188.09 m), indicating interesting changes in groundwater elevation. Straight contour lines from yellow to purple indicate a relatively consistent and flat distribution of groundwater elevation in the model. Higher groundwater elevations are represented by yellow colors, while lower elevations are represented by purple colors. The x and y axes on the plot indicate locations within the model, and their values influence the distribution of groundwater elevation in the model. Additionally, the values on the colorbar beside the plot, namely 0, 240, 400, 600, 800, and 1000, indicate the elevation scale in relevant units, which is meters.

Figure (c) shows that dolomite material influences the distribution of groundwater elevation in the model. On the plot, the color gradient ranges from yellow (9404.95 m) to green (7523.96 m), turquoise (5642.97 m), dark green (3761.98 m), and shades of purple (1880.99 m). Straight contour lines from yellow to purple indicate a relatively consistent and flat distribution of groundwater elevation in the model. Higher groundwater elevations are represented by yellow colors, while lower elevations are represented by purple colors. The x and y axes on the plot indicate locations within the model, and their values influence the distribution of groundwater elevation in the model. Additionally, the values on the colorbar beside the plot, namely 0, 2000, 4000, 6000, 8000, and 10000, indicate the elevation scale in relevant units, which is meters.

Figure (d) presents the simulation results for clay material with a hydraulic conductivity value of 0.0002 m/day. The plot illustrates a color gradient from around 47024.77 m (yellow) to 37619.82 m (green), then 28214.86 m (turquoise), followed by 18809.91 m (dark green to dark blue), and finally reaching approximately 9404.95 m (shades of purple). The x-axis values used in the plot are 0.00, 0.25, 0.50, 0.75, 1.00, 1.25, 1.50, and 1.75 m. Additionally, there is a colorbar next to the plot, indicating values of 0, 10000, 20000, 30000, 40000, and 50000 m. Contour lines on the plot reveal an intriguing pattern: straight contour lines from yellow indicate areas with higher and relatively flat groundwater elevations.

When conducting simulations with higher hydraulic conductivity, the model records higher groundwater elevations. Consequently, the highest values in the "Simulated Heads" plot will also be greater. The colorbar is used to represent the scale of groundwater elevation values, and with higher hydraulic conductivity, the range of values on the colorbar will be expanded to encompass higher groundwater elevations. Conversely, if hydraulic conductivity is lower, rocks or aquifers will have a reduced capacity to transmit water, leading to lower groundwater elevations within the model. In such cases, the range of values on the colorbar will be smaller and will encompass lower groundwater elevations.

Conclusion

Based on the results of this research, it can be concluded that the use of SEAWAT software enables accurate simulations of saltwater intrusion processes within an aquifer context. This study successfully simulated the distribution of salinity spread, observed groundwater flow patterns, and variations in groundwater elevation resulting from differences in material types and hydraulic conductivity within the hydrogeological model. These simulation results provide a deeper understanding of the factors influencing saltwater intrusion, including hydraulic conductivity and material characteristics. Among all the simulated results, saltwater intrusion occurred in cluster (d), where the hydraulic conductivity values for materials such as silt (0.08 m/day), clay (0.0002 m/day), dolomite (0.001 m/day), and basalt (0.01 m/day) were particularly low. In this scenario, saltwater intrusion entered from the central part of the model due to the low hydraulic conductivity, which limited groundwater flow within the model. Regarding groundwater elevations or "heads," among all the simulated results, the highest groundwater elevation was also found in cluster (d), where the range of groundwater elevations varied from 10,000 m to 50,000 m. Low values of hydraulic conductivity, such as 0.0002 m/day as simulated, impede groundwater flow and can lead to the accumulation of water, thereby increasing the water table. The importance of this understanding in groundwater resource management and aquifer management planning becomes evident. It contributes to efforts aimed at maintaining the sustainability of aquifer ecosystems and reducing the negative impacts of saltwater intrusion.

Acknowledgments

The authors are grateful to Rector of Unsrat for facilitating funding for this study through RDUU_K2 with SP DIPA-571/UN12.13/LT/2023.

Authors Contribution

Conceptualization, data curation, writing-original draft preparation, methodology, formal analysis, investigation, F., T.W., and D.P.P.; supervision, writing-review and editing, validation, visualization, M.D.B., H.F.S., A.T., S.H.T., and H.S.K. All authors have read and agreed to the published version of the manuscript.

Funding

This research is funding by RDUU_K2 with SP DIPA-571/UN12.13/LT/2023.

Conflicts of Interest

All authors declare that there is no conflict of interest.

References

Abd-Elaty, I., Abd-Elhamid, H. F., & Qahman, K. (2020). Coastal Aquifer Protection from Saltwater Intrusion Using Abstraction of Brackish Water and Recharge of Treated Wastewater: Case Study of the Gaza Aquifer. *Journal of Hydrologic Engineering*, *25*(7), 05020012. https://doi.org/10.1061/(asce)he.1943-5584.0001927

Abd-Elaty, I., Elhamid, H. F. A., & Javadi, A. (2016). Numerical Analysis of the Effects of Changing Hydraulic Parameters on Saltwater Intrusion in Coastal Aquifers. *Engineering Computations (Swansea, Wales)*, *33*(8), 2546–2564. https://doi.org/10.1108/EC-11-2015-0342

Ajami, H. (2021). Geohydrology: Groundwater. In *Encyclopedia of Geology* (2nd ed.). Elsevier Inc. https://doi.org/10.1016/b978-0-12-409548-9.12388-7

Ardaneswari, T. A., Yulianto, T., & Putranto, T. T. (2016). Analisis Intrusi Air Laut Meggunakan Data Resistivitas dan Geokimia Airtanah di Dataran Aluvial Kota Semarang. *Youngster Physics Journal*, *5*(4), 335-350. Retrieved from https://ejournal3.undip.ac.id/index.php/bfd/article/view/14116

Bakker, M., Schaars, F., Hughes, J. (2013). *Documentation of the Seawater Intrusion (SWI2) Package for MODFLOW*. https://doi.org/10.3133/tm6A46

Benz, S. A., Bayer, P., & Blum, P. (2017). Global Patterns of Shallow Groundwater Temperatures. *Environmental Research Letters*, *12*(3). https://doi.org/10.1088/1748-9326/aa5fb0

Bordbar, M., Neshat, A., Javadi, S., Pradhan, B., & Aghamohammadi, H. (2020). Meta-Heuristic Algorithms in Optimizing GALDIT Framework: A Comparative Study for Coastal Aquifer Vulnerability Assessment. *Journal of Hydrology*, *585*(March),124768. https://doi.org/10.1016/j.jhydrol.2020.124768

Cahyadi, T. A., Notosiswoyo, S., Iskandar, I., Widodo, L. E., & Suyono, S. (2014). Distribusi Konduktivitas Hidraulik dari Hasil Uji Akuifer-Constant Head Permeabilitas pada Batuan Sedimen Secara Heterogen. *Conference: Temu Profesi Tahunan (TPT) XXIII PERHAPI 2014*, 352-360. Makasar, Indonesia. http://dx.doi.org/10.17605/OSF.IO/AF8SN

Cantelon, J. A., Guimond, J. A., Robinson, C. E., Michael, H. A., & Kurylyk, B. L. (2022). Vertical Saltwater Intrusion in Coastal Aquifers Driven by Episodic Flooding: A Review. *Water Resources Research*, *58*(11), e2022WR032614. https://doi.org/10.1029/2022wr032614

Damayanti, C. (2020). Penerapan Metode Global untuk Identifikasi Daerah Intrusi Air Laut. *Seminar Nasional Riset Teknologi Terapan*, *1*(1). Retrieved from https://jurnal.untidar.ac.id/index.php/senaster/article/view/2547

Darsono, D., & Darmanto, D. (2019). Identifikasi Keberadaan Lapisan Akuifer Tertekan (Confined Aquifer) Berdasarkan Data Geolistrik (Studi Kasus: Desa Sambirejo Kecamatan Plupuh Kabupaten Sragen). *Indonesian Journal of Applied Physics*, *9*(01), 46. https://doi.org/10.13057/ijap.v9i01.30122

Diersch, H. J. G., & Kolditz, O. (2002). Variable-Density Flow and Transport in Porous Media: Approaches and Challenges. *Advances in Water Resources*, *25*(8-12), 899-944. https://doi.org/10.1016/S0309-1708(02)00063-5

Fahs, M., Koohbor, B., Belfort, B., Ataie-Ashtiani, B., Simmons, C. T., Younes, A., & Ackerer, P. (2018). A Generalized Semi-Analytical Solution for the Dispersive Henry Problem: Effect of Stratification and Anisotropy on Seawater Intrusion. *Water (Switzerland)*, *10*(2), 1–24. https://doi.org/10.3390/w10020230

Guo, W., & Langevin, C. D. (2002). *User's Guide to SEAWAT: A Computer Program for Simulation of Three Dimensional Variable-Density Ground-Water Flow*. U.S. Geological Survey Techniques of Water-Resources Investigations, book 6, chap. A7, 77 p.

Harding, R. (1991). *The Saline Groundwater of the Sow Valley, and of the Upper Trent Valley near Weston* (MSc Thesis). University of Birmingham, Birmingham.

Harbaugh, A. W. (2005). *MODFLOW-2005, the US Geological Survey Modular Ground-Water Model: the Ground-Water Flow Process*. U.S. Geological Survey.

Henry, H. R. (1964). *Effects of Dispersion on Salt Encroachment in Coastal Aquifers*. Sea Water in Coastal Aquifers, U.S. Geol. Surv. Supply Pap., 1613-C, C71-C84.

Hughes, J. D., & Sanford, W. E. (2004). *SUTRA-MS A Version of SUTRA Modified to Simulate Heat and Multiple-Solute Transport*. Water-Resources Open-File Report 2004-1207. Retrieved from https://pubs.usgs.gov/of/2004/1207/

Hunt, A. G., Skinner, T. E., Ewing, R. P., & Ghanbarian-Alavijeh, B. (2011). Dispersion of Solutes in Porous Media. *European Physical Journal B*, *80*(4), 411–432. https://doi.org/10.1140/epjb/e2011-10805-y

Kalangi, P. N., Mandagi, A., Masengi, K. W., Luasunaung, A., Pangalila, F. P., & Iwata, M. (2013). Sebaran Suhu dan Salinitas di Teluk Manado. *Jurnal Perikanan dan Kelautan Tropis*, *9*(2), 70–75. https://doi.org/10.35800/jpkt.9.2.2013.4179

Lee, H. (2018). *SEAWAT with Flopy - Density-driven flow simulation*. Retrieved from https://github.com/modflowpy/pymake

Lu, C., Chen, Y, Zhang, C., & Luo, J. (2013). Zona Pencampuran Air Tawar-Air Laut yang Stabil di Akuifer Pesisir Bertingkat. *J Hydrol*, *505*, 24–34. http://dx.doi.org/10.1016/j. jhydrol.2013.09.017

Manginsela, F. B., Rondo, M., Rondonuwu, A. B., Kambey, A. D., & Lumuindong, F. (2016). *Ekologi Perairan Teluk Manado*. Penerbit FPIK Unsrat.

Mei, T., Zendrato, K., & Har, R. (2021). Analisis Perhitungan Debit Air Tanah pada Sistem Penyaliran Tambang Terbuka di Pit X PT. Bukit Asam Tbk., Kabupaten Muara Enim, Provinsi Sumatera Selatan. *Jurnal Bina Tambang*, *6*(5).

Ouhamdouch, S., Bahir, M., & Ouazar, D. (2021). Seawater Intrusion into Coastal Aquifers from Semi-Arid Environments, Case of the Alluvial Aquifer of Essaouira basin (Morocco). *Carbonates and Evaporites*, *36*(1), 1–12. https://doi.org/10.1007/s13146-020-00663-9

Panguriseng, D. (2018). *Pengelolaan Air Tanah*. Yogyakarta: Pena Indis.

Posundu, R. S. A., Kepel, R. C., Mandagi, S. V., Kalalo, F. P., Paruntu, C. P., Mingkit, W. M., & Boneka, F. B. (2019). Study on Public Facilities Zone Development Strategy asTourism Support in Manado Bay. *Jurnal Ilmiah Platax*, *7*(1), 294-308. https://doi.org/10.35800/jip.7.1.2019.23404

Pu, L., Xin, P., Nguyen, T. T. M., Yu, X., Li, L., & Barry, D. A. (2020). Thermal Effects on Flow and Salinity Distributions in Coastal Confined Aquifers. *Water Resources Research*, *56*(10), 1–17. https://doi.org/10.1029/2020WR027582

Sarmauli, O., Setyawan, A., & JS, D. (2016). Identifikasi Potensi Akuifer Berdasarkan Metode Geolistrik Tahanan Jenis pada Daerah Krisis Air Bersih di Kota Semarang. *Youngster Physics Journal*, *5*(4), 327-334. Retrieved from https://ejournal3.undip.ac.id/index.php/bfd/article/view/14102

Shevah, Y. (2014). Adaptation to Water Scarcity and Regional Cooperation in the Middle East. In *Comprehensive Water Quality and Purification* (Pp. 40-70). Elsevier Ltd. https://doi.org/10.1016/B978-0-12-382182-9.00004-9

Simpson, M. J., & Clement, T. B. (2004). Improving the Worthiness of the Henry Problem as a Benchmark for Density-Dependent Groundwater Flow Models. *Water Resources Research*, *40*(1), W01504. http://dx.doi.org/10.1029/2003WR002199

Suhana, M. P. (2018). *Karakteristik Sebaran Menegak dan Melintang Suhu dan Salinitas*. Coastal and Marine Resources Research Center, Raja Ali Haji Maritime University Tanjungpinang-Indonesia.

Syaifullah, M. D. (2015). Suhu Permukaan Laut Perairan Indonesia dan Hubungannya dengan Pemanasan Global. *Jurnal Segara*, *11*(2), 37–47. http://dx.doi.org/10.15578/segara.v11i2.7356

Tamborski, J., Brown, C., Bokuniewicz, H., Cochran, J. K., & Rasbury, E. T. (2020). Investigating Boron Isotopes for Identifying Nitrogen Sources Supplied by Submarine Groundwater Discharge to Coastal Waters. *Frontiers in Environmental Science*, *8*(3), 1–15. https://doi.org/10.3389/fenvs.2020.00126

Thorne, D. T., Jr., Langevin, C. D., & Sukop, M. C. (2006). Addition of Simultaneous Heat and Solute

Transport and Variable Fluid Viscosity to SEAWAT. *Computer and Geosciences*, *32*(10), 1758-1768. http://dx.doi.org/10.1016/j.cageo.2006.04.005

Wals, J., & Westra, J. (2015). *Cases in Bioplanet Earth Overexploitation of Coastal Aquifers*. https://doi.org/10.13140/RG.2.1.2677.5523

Werner, A. D., Bakker, M., Post, V. E. A., Vandenbohede, A., Lu, C., Ataie-Ashtiani, B., Simmons, C. T., & Barry, D. A. (2012). Sea Water Intrusion Processes, Investigation and Management: Recent Advances and Future Challenges. *Advances in Water Resources*, *51*, 3-26. http://dx.doi.org/10.1016/j.advwatres.2012.03.004

Werner, A. D., & Simmons, C. T. (2009). Impact of Sea-Level Rise on Sea Water Intrusion in Coastal Aquifers. *Groundwater*, *47*(2), 197–204. https://doi.org/10.1111/j.1745-6584.2008.00535.x

Zhang, H., Xu, W. L., & Hiscock, K. M. (2013). Application of MT3dms and Geographic Information System to Evaluation of Groundwater Contamination in the Sherwood Sandstone Aquifer, UK. *Water, air, & Soil Pollution*, *224*(2), 1438. http://dx.doi.org/10.1007/s11270-013-1438-z